Correlation between magnetic state and bulk modulus of Cr_2AlC

Martin Dahlqvist, Björn Alling and Johanna Rosén

Original Publication:

Martin Dahlqvist, Björn Alling and Johanna Rosén, Correlation between magnetic state and bulk modulus of Cr_2AlC, 2013, Journal of Applied Physics, (113), 21.
http://dx.doi.org/10.1063/1.4808239

Correlation between magnetic state and bulk modulus of Cr_2AlC

M. Dahlqvist,[a] B. Alling, and J. Rosén
Thin Film Physics Division, Department of Physics, Chemistry, and Biology (IFM), Linköping University, SE-581 83 Linköping, Sweden

(Received 3 February 2013; accepted 15 May 2013; published online 5 June 2013)

The effect of magnetism on the bulk modulus (B_0) of M_2AlC (M = Ti, V, and Cr) has been studied using first principles calculations. We find that it is possible to identify an energetically favorable magnetic Cr_2AlC phase without using any adjustable parameter, such as the Hubbard U. Furthermore, we show that an in-plane spin polarized configuration has substantially lower B_0 as compared to the non-magnetic model. The existences of local magnetic moments on Cr atoms considerably improve agreement between theory and experiment regarding trends in B_0 for M_2AlC phases. © *2013 AIP Publishing LLC*. [http://dx.doi.org/10.1063/1.4808239]

The $M_{n+1}AX_n$ (MAX) phases ($n = 1$–3) are hexagonal inherently nanolaminated materials, where M is transition metal, A is an A-group element, and X is either C and/or N.[1–4] $M_{n+1}X_n$ layers are interleaved with layers of A elements, allowing these materials to combine the characteristics of ceramics and metals, including properties such as good electrical and thermal conductivity, high stiffness, excellent thermal shock resistance, and good corrosion resistance.[3,4] There has been a wide interest for obtaining magnetic $M_{n+1}AX_n$ phases, as their nanolaminated structure makes them promising for potential spintronic applications.[5–12] However, only recently the first magnetic phases were theoretically predicted and synthesized.[5,11,12] Furthermore, the ambiguity concerning a possible spin configuration of the well known Cr_2AlC phase remains to be theoretically resolved.[6,8,9]

Apart from importance in applications specifically requiring magnetism, the spin degree of freedom has shown potential for large impact on mechanical materials properties, such as the bulk modulus (B_0), not the least in Cr-based compounds.[13,14] The bulk modulus has been an issue for discussion in the MAX phase Cr_2AlC. In particular, it has been demonstrated that, in contrast to Ti_2AlC and V_2AlC, first principles calculations and experimental results deviate for B_0 of Cr_2AlC. This becomes particularly clear when comparing the theoretical and experimental trend in B_0 for M = Ti, V, and Cr in M_2AlC. An indirect method based on specific heat measurements indicates an increase in B_0 from Ti to Cr.[15] However, more direct experiments, e.g., diamond anvil cell, show an increase in B_0 when the M-element is changed from Ti to V, but a *decrease* from V to Cr.[16,17] Density functional theory (DFT) calculations based on generalized gradient approximation (GGA) or local density approximation (LDA), on the other hand, display an almost monotonously increase in B_0 along the Ti-V-Cr series.[10,15,18,19] The origin of this discrepancy has been investigated: Temperature effects of Cr_2AlC have been studied using ab initio molecular dynamics (MD), resulting in a small decrease of B_0 (15%) from 248 GPa at 0 K to 212 GPa at 1200 K, despite no explanation for the experimental trend observed at room temperature for all three MAX phases.[20] In attempts to identify the Cr_2AlC ground state, several groups have searched for possible spin polarization of Cr atoms in Cr_2AlC. Considering a small set of ferro-, antiferro-, and non-magnetic configurations (FM, AFM, and NM, respectively), a NM solution has been predicted for this material.[9,10] Recently, the DFT+U method was used motivated by the underestimated volume of Cr_2AlC in GGA calculations due to electron correlation effects.[6,8] Only by using the DFT+U method Ramzan *et al.*[8] were able to stabilize magnetic states. Even though strong electron correlations beyond the description of GGA/LDA are potentially interesting for many systems, the MAX phases have previously been shown to be well described by GGA with respect to both phase stability and structural properties.[21–25]

In this work, we stay within the GGA description of electron correlations and extend the range of considered magnetic configurations beyond what has previously been reported for MAX phases. We show that it is possible to theoretically identify a magnetic ground state of Cr_2AlC without any adjustable parameter, such as the Hubbard U, and that this spin polarized configuration has substantially lower bulk modulus as compared to the non-magnetic model. In fact, we find that there are several possible AFM spin polarized configurations which should be considered in the calculations of mechanical properties and stability of potentially magnetic MAX phases.

All calculations were performed using the projector augmented-wave (PAW) method[26] as implemented within VASP.[27,28] Exchange and correlation effects were treated in the framework of the Perdew-Burke-Ernzerhof (PBE)[29] GGA in its spin-polarized form. We have used a plane wave energy cutoff of 400 eV, and integration of the Brillouin zone was performed using the Monkhorst-Pack scheme[30] with $23 \times 23 \times 7$ and $13 \times 23 \times 7$ k-point mesh for $1 \times 1 \times 1$ and $2 \times 1 \times 1$ unit cells, respectively. Optimal geometries were obtained by structural optimization in terms of volume, c/a ratios, and internal parameters. Bulk modulus was determined by fitting the energy-volume values with a Birch-Murnaghan equation of state.

For a FM configuration all M atoms have the same spin orientation. However, for an AFM state, the set of possible configurations are many although, in practice, limited to

[a]Author to whom correspondence should be addressed. Electronic mail: madah@ifm.liu.se

configurations that maximize the number of anti-parallel moments on a few nearest neighbor shells. We consider 5 different collinear AFM configurations as well as the FM and the NM approach, as shown in Fig. 1. Notice that for some AFM configurations, the original unit cell $(1 \times 1 \times 1)$ with 8 atoms is insufficient and needs to be expanded into an in-plane supercell of at least $2 \times 1 \times 1$ in order to have opposite spins for M atoms within the same layer. Three AFM configurations are considered for the $1 \times 1 \times 1$ unit cells: double layered [0001] AFM ordering with spins changing sign upon crossing an A or an X atom ($\mathrm{AFM}[0001]_2^A$ and $\mathrm{AFM}[0001]_2^X$, respectively) and single layer $[0001]_1$ AFM ordering with spins changing sign for every [0001]-layer of M-atoms ($\mathrm{AFM}[0001]_1$). The notations for supercells $(2 \times 1 \times 1)$ with in-plane AFM are in-AFM1 and in-AFM2.

The different magnetic configurations in Fig. 1 can be defined using spin correlation functions Φ_α to describe the applied spins in different coordination shells α of the M atoms. The definition of the spin correlation functions, the average relative orientations of the magnetic moments in the α:th coordination shell of the M atoms, is given by $\Phi_\alpha = \frac{1}{N}\sum_{i,j\in\alpha} \mathrm{e}_i \cdot \mathrm{e}_j$, where N is the number of terms in the sum and $\mathbf{e}_i$ and $\mathbf{e}_j$ are unit vectors in the direction of the local magnetic moment on site i and j. In our collinear case, the spins are parallel and/or antiparallel to each other with unit vectors $\mathbf{e}_i$ and $\mathbf{e}_j$ of either $+1$ for spin up or -1 for spin down. For $\Phi_\alpha = 1$ all atoms in shell α have the same spin direction as the center atom ($\mathbf{e}_i = \mathbf{e}_j$) whereas $\Phi_\alpha = -1$ corresponds to an antiparallel configuration with opposite spin direction of all neighboring spins in shell α. When $\Phi_\alpha = 0$ there are equal amount of parallel and anti parallel spin pairs in coordination shell α, which is the case for an ideally random distribution of spins. For Cr_2AlC, the first four coordination shells are defined in Fig. 1, and the corresponding correlation function Φ_α, together with the coordination number in these shells, needed to separate the six different magnetic configurations are shown in Fig. 1.

By including antiparallel spins within the same Cr-layer, the spin correlation function Φ_α for in-AFM1 and in-AFM2 differs from previously studied configurations in the first and second coordination shells, $\Phi_{1,2} \neq \pm 1$. In terms of relative stability in-AFM1 is found to be the ground state with an energy of -11.0 meV/f.u as compared to NM configuration. It has local magnetic moments of $\pm 0.70\,\mu_B$/Cr. The in-AFM2 configuration also shows non-zero magnetic moment on Cr but is slightly higher in energy. Worth noting is that FM, $\mathrm{AFM}[0001]_2^A$, $\mathrm{AFM}[0001]_2^X$, and $\mathrm{AFM}[0001]_1$ are degenerated with NM with no magnetic moment on Cr. Hence, by considering several AFM configurations, we have found, in contrast to previous works, a spin-polarized configuration to be the lowest in energy for Cr_2AlC. We have also applied the above mentioned magnetic configurations on Ti_2AlC and V_2AlC without any effect on the total energy and with resulting zero magnetic moment, i.e., states converging towards NM.

We now turn to the impact of the obtained antiferromagnetic state on the bulk modulus B_0 of Cr_2AlC. In Figure 2, experimental[16,17] and calculated[10,15,18,19] B_0 of M_2AlC is shown for M = Ti, V, and Cr. B_0 increases when going from Ti_2AlC to V_2AlC. However, experiments show a clear decrease in B_0 when going from V_2AlC to Cr_2AlC; previous theoretical work consistently shows a corresponding continued increase. Using our identified lowest energy magnetic configuration (in-AFM1), we calculate for Cr_2AlC a B_0 that is decreasing as compared to V_2AlC. This result, filled squares in Fig. 2(b), diverges from earlier theoretical work but are in line with the trend observed experimentally. We have also included here the calculated B_0 of 188 GPa for NM Cr_2AlC (open squares in Fig. 2(b)) to visualize the decrease of 17 GPa ($\sim -10\%$) to 171 GPa upon onset of magnetization in the in-AFM1 configuration.

Efforts have been made to model paramagnetic (PM) Cr_2AlC approximated by means of the disorder local moment (DLM) model.[31,32] This was achieved by simulating a solid solution with 50% up Cr↑ and 50% down Cr↓ spins on the M sublattice, using the special quasirandom structures method.[33] However, in attempts to model PM Cr_2AlC with such a disordered initial spin configuration, a semi-ordered spin state is obtained after electronic relaxation attempts, resembling in-AFM1. Thus, local moments survive disordering attempts, underlining their importance for B_0 also in the PM regime. However, more advanced magnetic simulations beyond the Heisenberg picture is needed to estimate the Néel temperature of this material.

Atoms along c-axis	FM	$\mathrm{AFM}[0001]_2^A$	$\mathrm{AFM}[0001]_2^X$	$\mathrm{AFM}[0001]_1$	in-AFM1	in-AFM2
C						
Cr						
Al						
Cr						
C						
Cr						
Al						
Cr						
C						
$\Phi_{1,2,3,4}$ (n_α = 3,6,3,1)	1,1,1,1	1,1,1,−1	−1,1,−1,1	−1,1,−1,−1	−1/3,−1/3,1,1	1/3,−1/3,−1,1
E-E^{NM} (meV/f.u.)	0.0	0.0	0.0	0.0	−11.0	0.6

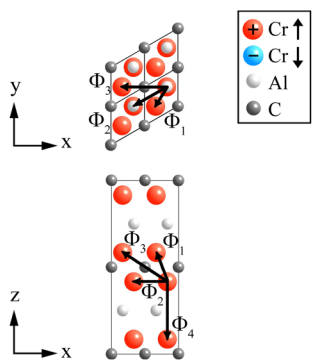

FIG. 1. Schematic illustration of different magnetic configurations for Cr_2AlC with spin correlation functions Φ_α for the first four coordination shells. The term n_α is the number of atoms in shell α. Corresponding energy differences relative to NM configuration are also shown. The right-hand side shows the unit vectors for the first four spin coordination shells.

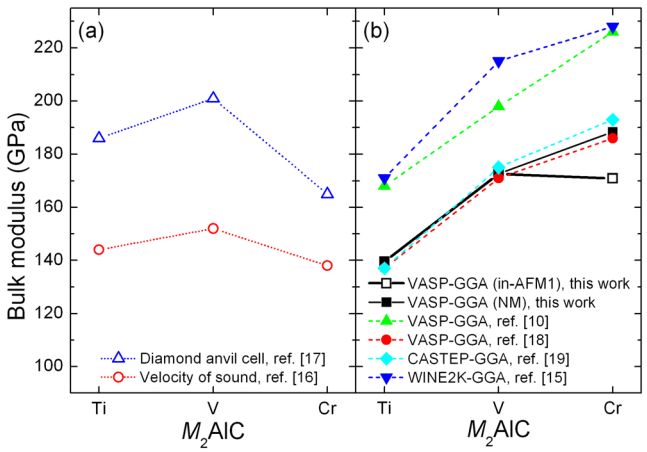

FIG. 2. Bulk modulus B_0 for M_2AlC, where M = Ti, V, and Cr, from (a) published experimental data (open symbols with dotted lines), (b) our calculated data (square symbols with solid lines), and previously published theoretical results (solid symbols with dashed lines).

Moreover, the lattice parameters for in-AFM1 Cr_2AlC are improved relative to NM Cr_2AlC, as seen in Table I, and our values for M_2AlC (M = Ti, V, and Cr) are in good agreement with experimental results. For comparison, previous calculated[10,19] and experimental[17,34] lattice parameters of M_2AlC (M = Ti, V, and Cr) is shown in Table I.

The results presented within this work show that the original unit cell of 8 atoms is insufficient for describing antiferromagnetic ordering in Cr-containing 211 MAX phases. By expanding to 16 atoms per unit cell ($2 \times 1 \times 1$ supercell) it is possible to simulate antiferromagnetism within a M-layer, corresponding to the second M-atom correlation shell, and obtain magnetic configurations stabilizing the structure and significantly affecting materials properties like the bulk modulus. No adjustable parameters have been used in the present calculations. However, use of, e.g., GGA+U may be suitable for improved description of the electronic correlation in Cr-based phases although evidently it is not necessary for predicting a stable magnetic state. Hence, it should be noted that magnetic ordering in MAX phases is non-trivial and that it is important to allow for a broad range of AFM configurations. The existence of local magnetic moments on Cr-atoms, also within a traditional GGA approach, is shown to considerably improve agreement between theory and experiment regarding trends in bulk modulus for M_2AlC MAX phases.

TABLE I. Calculated and experimental lattice parameters of M_2AlC (M = Ti, V, and Cr) with our values in bold.

Phase	Method	a (Å)	c (Å)
Ti_2AlC	Calc.	**3.069**, 3.06,[a] 3.053[b]	**13.728**, 13.67,[a] 13.64[b]
	Expt.	3.065,[c] 3.052[d]	13.71,[c] 13.64[d]
V_2AlC	Calc.	**2.906**, 2.95,[a] 2.895[b]	**13.110**, 13.29,[a] 13.015[b]
	Expt.	2.914,[c] 2.909[d]	13.19,[c] 13.12[d]
Cr_2AlC	Calc. (NM)	**2.844**, 2.85,[a] 2.822[b]	**12.707**, 12.72,[a] 12.590[b]
	Calc. (in-AFM1)	**2.850**	**12.727**
	Expt.	2.857,[c] 2.854[d]	12.81,[c] 12.82[d]

[a]Reference 10.
[b]Reference 19.
[c]Reference 17.
[d]Reference 34.

The research leading to these results has received funding from the European Research Council under the European Community Seventh Framework Program (FP7/2007-2013)/ERC Grant Agreement No. 258509. J.R. and B.A. also acknowledge funding from the Swedish Research Council (VR) (Grant Nos. 621-2012-4425 and 621-2011-4417). The calculations were carried out using supercomputer resources provided by the Swedish National Infrastructure for Computing (SNIC).

[1]H. Nowotny, Prog. Solid State Chem. **5**, 27 (1971).
[2]M. W. Barsoum and T. El-Raghy, J. Am. Ceram. Soc. **79**, 1953 (1996).
[3]M. W. Barsoum, Prog. Solid State Chem. **28**, 201 (2000).
[4]P. Eklund, M. Beckers, U. Jansson, H. Högberg, and L. Hultman, Thin Solid Films **518**, 1851 (2010).
[5]M. Dahlqvist, B. Alling, I. A. Abrikosov, and J. Rosen, Phys. Rev. B **84**, 220403 (2011).
[6]Y. L. Du, Z. M. Sun, H. Hashimoto, and M. W. Barsoum, J. Appl. Phys. **109**, 063707 (2011).
[7]W. Luo and R. Ahuja, J. Phys.: Condens. Matter **20**, 064217 (2008).
[8]M. Ramzan, S. Lebègue, and R. Ahuja, Phys. Status Solidi (RRL) **5**, 122 (2011).
[9]J. M. Schneider, Z. Sun, R. Mertens, F. Uestel, and R. Ahuja, Solid State Commun. **130**, 445 (2004).
[10]Z. Sun, R. Ahuja, S. Li, and J. M. Schneider, Appl. Phys. Lett. **83**, 899 (2003).
[11]A. S. Ingason, A. Mockute, M. Dahlqvist, F. Magnus, S. Olafsson, U. B. Arnalds, B. Alling, I. A. Abrikosov, B. Hjörvarsson, P. O. Å. Persson, and J. Rosen, Phys. Rev. Lett. **110**, 195502 (2013).
[12]A. Mockute, M. Dahlqvist, J. Emmerlich, L. Hultman, J. M. Schneider, P. O. Å. Persson, and J. Rosen, Phys. Rev. B **87**, 094113 (2013).
[13]F. Rivadulla, M. Banobre-Lopez, C. X. Quintela, A. Pineiro, V. Pardo, D. Baldomir, M. A. Lopez-Quintela, J. Rivas, C. A. Ramos, H. Salva, J.-S. Zhou, and J. B. Goodenough, Nature Mater. **8**, 947 (2009).
[14]B. Alling, T. Marten, and I. A. Abrikosov, Nature Mater. **9**, 283 (2010).
[15]S. E. Lofland, J. D. Hettinger, K. Harrell, P. Finkel, S. Gupta, M. W. Barsoum, and G. Hug, Appl. Phys. Lett. **84**, 508 (2004).
[16]J. D. Hettinger, S. E. Lofland, P. Finkel, T. Meehan, J. Palma, K. Harrell, S. Gupta, A. Ganguly, T. El-Raghy, and M. W. Barsoum, Phys. Rev. B **72**, 115120 (2005).
[17]B. Manoun, R. P. Gulve, S. K. Saxena, S. Gupta, M. W. Barsoum, and C. S. Zha, Phys. Rev. B **73**, 024110 (2006).
[18]M. F. Cover, O. Warschkow, M. M. M. Bilek, and D. R. McKenize, J. Phys.: Condens. Matter **21**, 305403 (2009).
[19]J. Wang and Y. Zhou, Phys. Rev. B **69**, 214111 (2004).
[20]J. M. Schneider, D. P. Sigumonrong, D. Music, C. Walter, J. Emmerlich, R. Iskandar, and J. Mayer, Scr. Mater. **57**, 1137 (2007).
[21]Y. C. Zhou, Z. Sun, X. Wang, and S. Chen, J. Phys.: Condens. Matter **13**, 10001 (2001).
[22]M. Magnuson, J. P. Palmquist, M. Mattesini, S. Li, R. Ahuja, O. Eriksson, J. Emmerlich, O. Wilhelmsson, P. Eklund, H. Högberg, L. Hultman, and U. Jansson, Phys. Rev. B **72**, 245101 (2005).
[23]D. Music, R. Ahuja, and J. M. Schneider, Appl. Phys. Lett. **86**, 031911 (2005).
[24]M. Dahlqvist, B. Alling, I. A. Abrikosov, and J. Rosén, Phys. Rev. B **81**, 024111 (2010).
[25]M. Dahlqvist, B. Alling, and J. Rosén, Phys. Rev. B **81**, 220102 (2010).
[26]P. E. Blöchl, Phys. Rev. B **50**, 17953 (1994).
[27]G. Kresse and J. Hafner, Phys. Rev. B **48**, 13115 (1993).
[28]G. Kresse and J. Hafner, Phys. Rev. B **49**, 14251 (1994).
[29]J. P. Perdew, K. Burke, and M. Ernzerhof, Phys. Rev. Lett. **77**, 3865 (1996).
[30]H. J. Monkhorst and J. D. Pack, Phys. Rev. B **13**, 5188 (1976).
[31]B. Alling, T. Marten, and I. A. Abrikosov, Phys. Rev. B **82**, 184430 (2010).
[32]B. L. Gyorffy, A. J. Pindor, J. Staunton, G. M. Stocks, and H. Winter, J. Phys. F: Met. Phys. **15**, 1337 (1985).
[33]A. Zunger, S. H. Wei, L. G. Ferreira, and J. E. Bernard, Phys. Rev. Lett. **65**, 353 (1990).
[34]J. C. Schuster, H. Nowotny, and C. Vaccaro, J. Solid State Chem. **32**, 213 (1980).